Hindawi
Mathematical Problems in Engineering
Volume 2019, Article ID 7306841, 13 pages
https://doi.org/10.1155/2019/7306841

Research Article

The Grey Theory Combining the Taguchi Method for the Best Parameters: A Case Study of Polishing M300 Steel

Xiaojun Wu, Yang Yang, Xin Tong, Xiao Shu, and Yan Li

School of Mechanical and Electrical Engineering, Xi'an University of Architecture and Technology, Xi'an, China

Correspondence should be addressed to Xiaojun Wu; wuxiaojun@xauat.edu.cn

Received 24 December 2018; Revised 17 February 2019; Accepted 25 February 2019; Published 13 March 2019

Academic Editor: Juan C. Jauregui-Correa

M300 steel, as high-chromium alloy steel with strong wear resistance and corrosion resistance, is widely used in the manufacture of complex profile molds and aerospace military equipment such as missile parts. However, there are still some problems such as the contradiction between productivity and surface quality in the polishing process for M300 steel. Therefore, in order to solve these problems, surface polishing experiments on M300 steel, single-factor and orthogonal experiments, and parameters' optimization were studied. In this paper, orthogonal experiments are conducted for four selected machining parameters: grain size (A), grinding speed (B), cutting depth (C), and feed rate (D) on a grinding machine. The experiment and parameters' optimization of the ball type abrasive tool polishing M300 were investigated by a five-axis machining center, electronic analytical balance, and three-dimensional surface topographer, and the optimal process parameters and preferred intervals were optimized. The optimal parametric condition obtained for simultaneous minimization of surface roughness (Ra) and maximization of material removal rate (MRR) is as follows: grain size=#320, grinding speed=4500 r/min, cutting depth=0.4 mm, and feed rate=80 mm/s. The above parametric combination has been validated by confirmatory tests.

1. Introduction

M300, high-chromium alloy steel, possessing several excellent properties including corrosion resistance and wear resistance, is a popular material in molds with complex surfaces and aerospace military equipment such as the key components of a missile carrier. However, due to high hardness, brittleness, and poor thermal conductivity in the finishing process, machining of M300 is time-consuming and inefficient [1] for the surface of the products requiring mirror roughness, which greatly affects the performance of the product.

In order to improve machining efficiency, reduce the machining cost, and improve the quality of machined parts, it is necessary to select the most appropriate processing method [2]. Polishing has proven to be a viable process for achieving the required mirror roughness of the products' surface. However, in order to reach these quality levels, polishing has to be done in the optimum condition, whereas achieving optimum conditions for polishing is difficult due to too many adjustable machining parameters. In order to minimize these machining problems, there is a need to utilize scientific methods to select cutting conditions for polishing of materials.

In recent years, superfinishing has received special attention due to its higher material removal rate (MRR), better part quality, and relatively low manufacturing costs [3]. To date, the superfinishing of simple profile workpieces with hard alloys has had a more mature process and equipment [4–6]. However, it is difficult using traditional manual polishing methods to acquire high-quality workpiece surfaces on microminiature surfaces to meet the modern processing and manufacturing requirements of low cost, short cycle, and high-quality [7, 8]. In order to cope with the contradiction between surface quality and processing efficiency in surface polishing, extensive research on mechanical polishing has been conducted by scholars at home and abroad in recent years, and great breakthroughs have been made. Zeng et al. [9] established a prediction model of the elastic abrasive material removal rate with respect to the grinding wheel rotation speed, offset, and precession angle based on the modified Preston equation. The reliability of the premodel was verified by polishing the medical cobalt-chromium alloy.

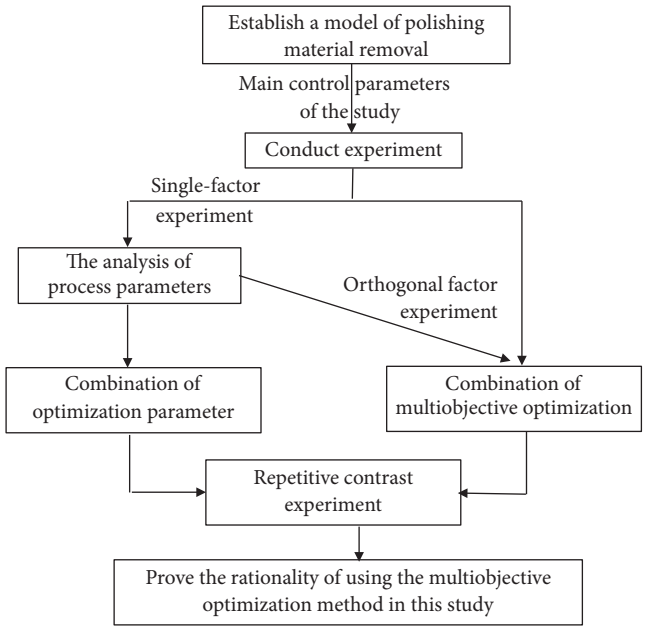

Figure 1: A flowchart of the entire research process.

Sooraj et al. [10] used a soft-bonded elastic abrasive tool to carry out the polishing experiment on the inner wall of the tube to investigate the effects of the material removal rate and surface roughness by particle size, contact pressure, and linear velocity. Wei Wei [11] performed grinding and polishing experiments on laser-enhanced high-hardness surfaces by the use of a progressive abrasive-grained pneumatic wheel, which effectively reduced the wear of the abrasive tools and obtained good surface quality. Xu Zaokun [12] achieved automatic mirror polishing of the inner and outer surfaces of stainless steel thin-walled parts by a variety of particle size elastic grinding wheels, of which they used the indicators of material removal rate and surface roughness to optimize the processing parameters.

The above research mainly analyzes the influence of grinding and polishing parameters on individual indexes such as material removal rate and surface quality of the workpiece. However, there are few researches on the optimization of grinding and polishing processing for multiple indexes, and there is still no complete experimental research on grinding and polishing processing on M300 materials. In view of the current problems and deficiencies in the processing of M300 steel, this paper investigated the removal mechanism of the ball type abrasive tool and the optimization of the relevant grinding parameters by using the ball type abrasive tool in superfinishing the surface of M300 in order to provide theoretical and technical support of the theory and process planning methods for the surface polishing of the ball type abrasive tool. Figure 1 is a flowchart of the entire research process.

This paper has the following sections:

Section 1 provides the general introduction. Section 2 analyzes the working mechanism of the elastic abrasive. Sections 3 presents the experimental work and experimental design. In Section 4, results are analyzed and compared.

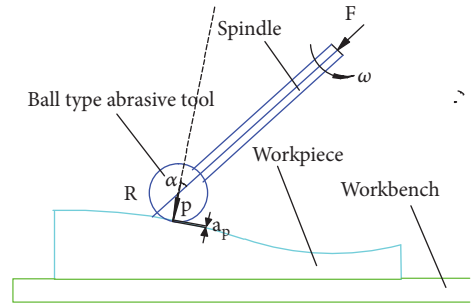

Figure 2: Contact diagram of spherical grinding head and complex curved surface.

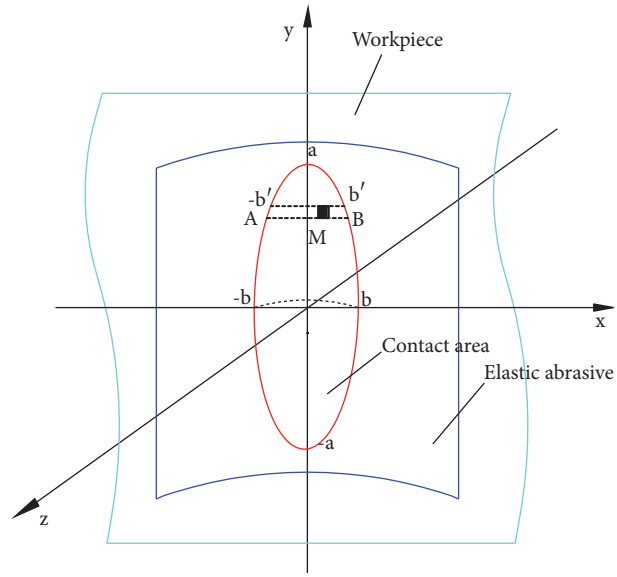

Figure 3: Contact status of spherical grinding head and workpiece surface.

2. Analysis of Working Mechanism of Elastic Abrasives

The contact diagram of the ball type abrasive tool and curved surface to be processed was shown in Figure 2. The polishing tool, under the press of F_n, is rotating with the speed of ω to polish the surface of the curved workpiece. And the precession angle, between the main direction of the main shaft of the elastic abrasive and the normal direction of the surface, is α.

In this research, the ball head portion of the polishing tool is made up of small particles of corundum covered with a binder. When the polishing tool comes into contact with the workpiece, it can be considered as an elastic deformable sphere pressed against a rigid flat. The simplified polishing process was the contact between the elastic sphere and the rigid curved surface. According to the Hertz theory, as shown in Figure 3, the contact faces of the two were approximately elliptical, and the pressure between the contact

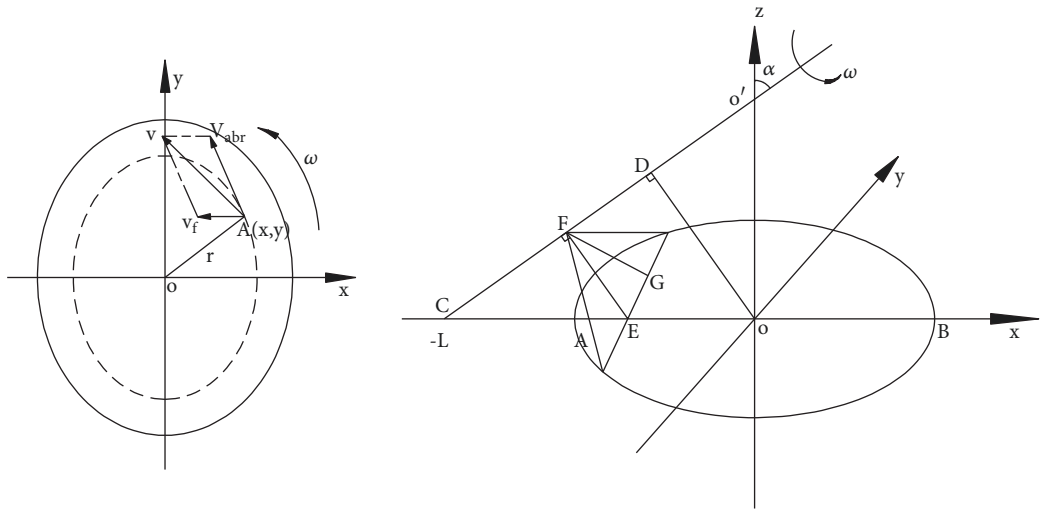

Figure 4: Speed vector diagram of the contact area between the workpiece and the ball head.

faces obeyed the elliptical Hertz distribution [12]; the pressure was calculated by

$$\mathrm{p}(x, y) = p_0 \sqrt{1 - \left(\frac{y}{a}\right)^2 - \left(\frac{x}{b}\right)^2}, \tag{1}$$

where P_0 is center pressure of the contact area (pa), $p_0 = 3F_n/2\pi ab$; F_n is the grinding and polishing pressure (N).

As a carrier of various grinding and polishing processes, the material removal mechanism has been extensively studied. Preston [13] proposed the well-known Preston equation, which assumes that the abrasive removal depth is proportional to the contact pressure and relative velocity. As shown in Figure 2, according to this assumption, material removal rate per unit length M can be expressed by

$$\frac{dh}{dl} = k_p \cdot \frac{v_s + v_f}{v_f} \cdot p, \tag{2}$$

where K_p is the correction factor, related to factors such as the hardness of the grinding tool and the workpiece; Vs is the tangential speed of abrasive point (mm/s); V_f is the feed rate of the grinding tool along the workpiece (mm/s); P is the contact pressure between the polishing tool and the workpiece (Pa).

Figure 3 schematically shows the details of the velocity distribution of a random point A(x,y) in the contact area when the polishing tool is rotating with the speed of ω. As shown in Figure 4, O is the center of the polished contact area, and its speed was calculated by

$$v_{os} = \omega \cdot \left|OO'\right| \cdot \cos\alpha. \tag{3}$$

Therefore, the speed of any point A(x, y) in the contact surface was calculated by

$$v_s(x, y) = \omega \cdot \sqrt{[(R - h)\sin\alpha + x\cos\alpha]^2 + y^2}. \tag{4}$$

The material removal amount of the contact region A-B along the X-direction point M could be obtained by integrating (2) on the range (-b′, b′):

$$h(x) = \int_{-b'}^{b'} \frac{dh}{dl} dy = \int_{-b'}^{b'} k_p \cdot p \cdot \frac{v_s + v_f}{v_f} dx. \tag{5}$$

Bring (1) and (5) into (2) to obtain the removal equation of the surface material in the contact region:

$$h(x) = -k_p \cdot \frac{v_s \pm v_f}{v_f} \cdot \frac{3F_n}{4a}\left[1 - \left(\frac{x}{a}\right)^2\right]. \tag{6}$$

As shown in (6), the surface material removal rate was affected by the feed speed (V_f), the spindle tangential movement speed (V_s), and the polishing pressure (F_n). Among them, if the precession angle is kept constant, Vs was specifically expressed as the grinding speed (W_t). For the elastic abrasive, the polishing pressure (F_n) was linearly proportional to the cutting depth (a_p) [14, 15] approximately. Therefore, the main control parameters of the elastic abrasive polishing process in this study were as follows: grinding speed W_t, cutting depth ap, feed rate V_f, and grain size S.

3. Experimental Details

3.1. Materials. The cuboid with only one surface curved that is utilized in this experiment had a length of 20 mm, a width of 14 mm, and a height of 100 mm. The experiment was carried out on the 20×100 curved face, which had a curvature of $0.21\,\mathrm{cm}^{-1}$. The chemical composition of the workpiece was listed in Table 1. The bar specimens were treated by a premilling process before the polishing experiment in order to obtain the desired surface roughness of about $1\,\mu$m. The ball type abrasive tool used in this study is as shown in Figure 5.

3.2. Design of Experiment. The experiment was investigated at the HSC 75 Linear Five-Axis Machining Center. The

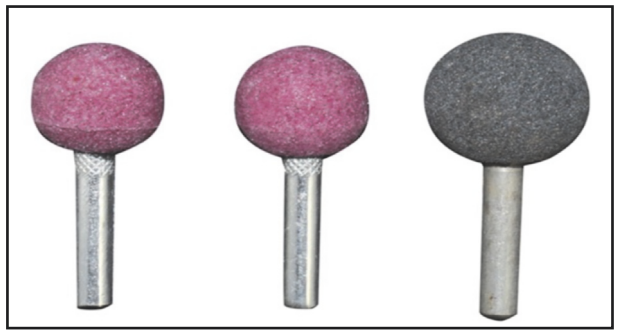

Figure 5: The ball type abrasive tool.

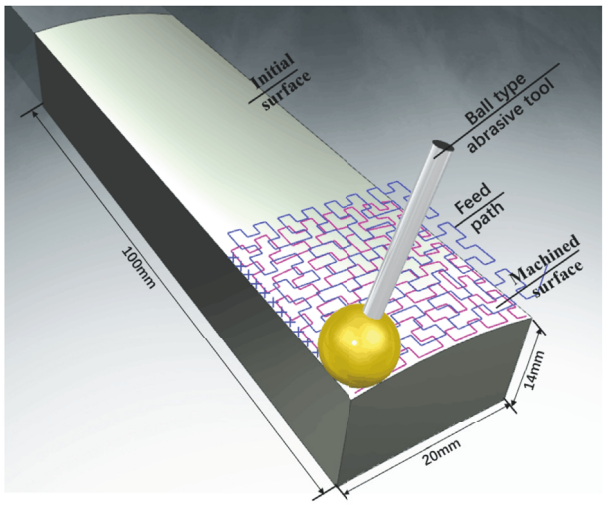

Figure 6: Feeding track of the ball type abrasive tool.

X, Y, and Z axis strokes of the machining center are 885 mm, 600 mm, and 600 mm; the B axis can achieve a rotation angle of +10 to 110°, and the C axis rotates 360 degrees. The linear axis achieves fast moving at a speed of 90 m/min.

This paper sets the Hilbert curve as the feed path to carry out the experiments. Since the elastic abrasive is required to polish the entire surface evenly in the superfinishing stage, a simple single-way and reciprocating path cannot meet such high polishing requirement. In order to fulfill this requirement, the Hilbert curve with disorder and uniform ergodicity [16] was used. The feed path is as shown in Figure 6.

The ball type abrasive tool used in this paper had a diameter of 10 mm to perform a single-factor experiment on the curve surface of the workpiece and design orthogonal experiment based on the Taguchi method [17]. Under the setting of polishing line spacing to 0.5 mm and precession angle α to 15°, a series of experiments were performed in order to study the influence of the cutting depth (a_p), the grinding speed (W_t), the feed rate (V_f), and the grain size (S) on the polishing process. The single-factor experiment parameters, the orthogonal factor experiment levels, and the orthogonal experiment results were shown in Tables 2–4.

Table 1: Chemical composition of M300 steel (wt%).

Material	C	Cr	Mo	Mn	Si	V	S
M300	1.4	11.5	1.0	0.4	0.3	0.3	0.002

Table 2: Experimental parameters for polishing.

Name	Condition	Unit
Abrasive and grain size	320#, 600#, 1000#	/
Grinding speed	1500-12000	r/min
Feed rate	20-160	mm/s
Cutting depth	0.05-0.4	mm
Polishing time	30-240	s
Polishing line spacing	0.5	mm

3.3. Measurement Methods. The surface quality of the workpiece and the elastic abrasive tool was measured using an Alicona InfiniteFocus three-dimensional shape analyzer instrument. At the start and the end of the experiment, the workpiece and the abrasive tool were dried after cleaning with an ultrasonic cleaner for 20 minutes, and then their quality was measured using a precision electronic analytical balance with an accuracy of 0.1 mg. In order to reduce the influence of random factors, the test results measured in those trials are the mathematical average of three measurements.

4. Results and Discussion

4.1. Effect from Different Grinding Parameters on the Process

4.1.1. On Material Removal Rate. In general, the polishing parameters, affecting the material removal ability of the ball type abrasive tool, were the cutting depth (a_p) and the spindle speed (W_t).

First of all, the effect of polishing parameters on MRR has been shown in Figure 7. Figure 7(a) describes a nonlinear decline of material removal rate (MRR) as the processing time increases. Three lines show the same trend on different feed rates with increasing the cutting speed. As is observed, under the same conditions, the MRR became higher with the grain size (S) smaller. The reason is that, in the early stage of processing, the sharper abrasive grains made more grains involved in cutting to improve the material removal rate. With the polishing process progressed, the abrasive grains became smooth and the material removal rate decreased. Under the same conditions, the abrasive tools with large grain size had more abrasive grains participating in cutting. Due to the less pressure suffered by single abrasive particles, more abrasive grains were in the stage of sliding and ploughing [14], and the overall material removal ability reduced.

In Figure 7(b), the material removal rate increased with the increase in grinding speed (w_t) from 1500 r/min to 12000 r/min. Figure 7(b) shows that the effect of grinding speed of the grain size of #320 is very significant on the material removal rate. Since the contact time between the abrasive grains and the workpiece declined by the increase in grinding speed, the cutting effects were

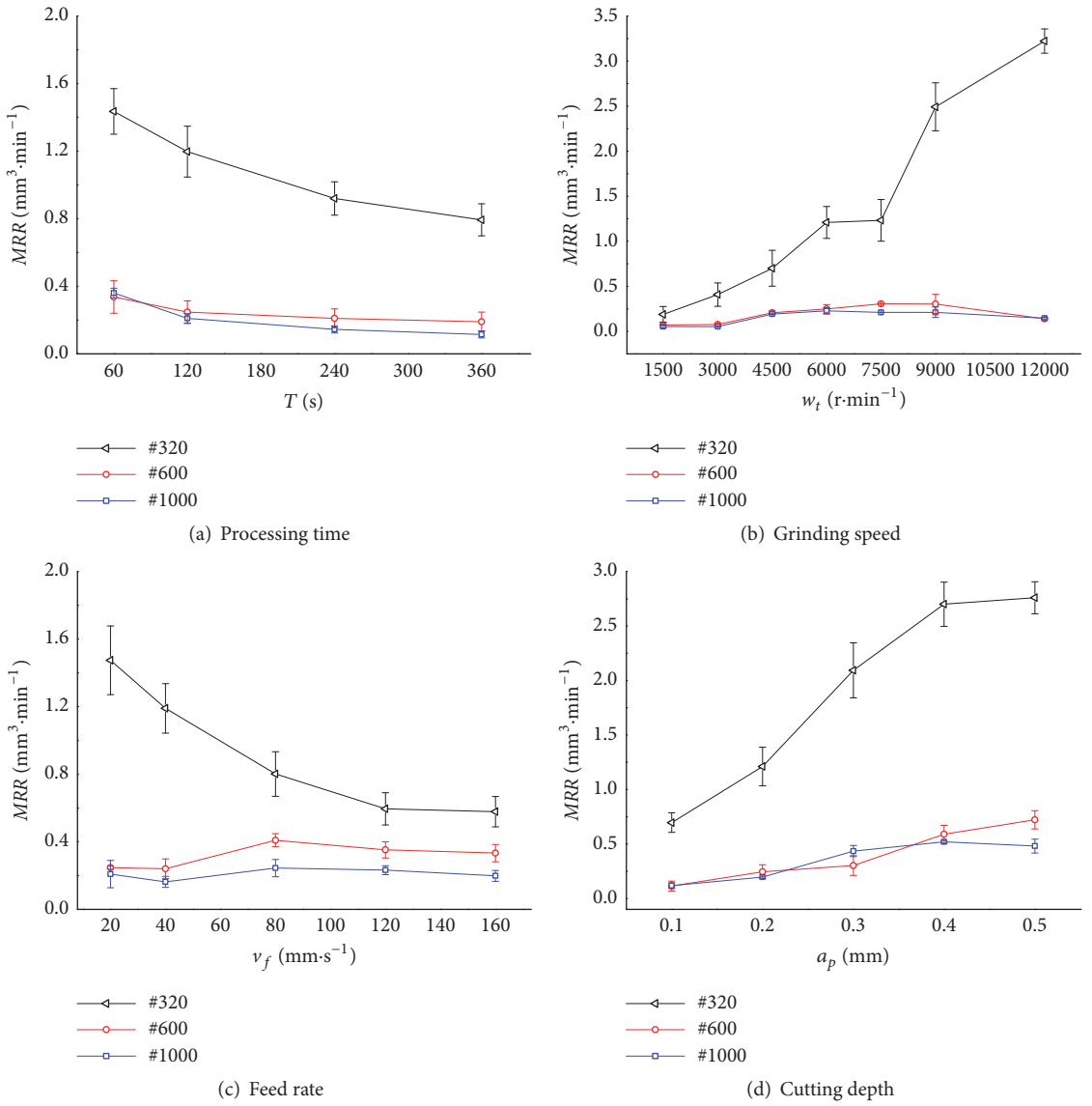

Figure 7: Plots of polishing parameters' effect on MRR.

Table 3: Factors and levels of the polishing parameter optimization experiment.

	Process parameter	Unit	Level		
			1	2	3
A	Grain size	/	320	600	1000
B	Grinding speed	r·min^{-1}	4500	6000	7500
C	Cutting depth	mm	0.1	0.2	0.4
D	Feed rate	mm/s	40	80	160
	Polishing line spacing			1	
	Processing cycles			3	

greater than the sliding and ploughing, the removal ability was increased, and the material removal rate was heightened.

However, a different trend is shown in Figure 7(c). The effect of feed rate of the grain size of #320 is very significant on the material removal rate (MRR); the MRR declined with the increase in feed rate (V_f) from 20 mm/s to 160 mm/s, while, for the grain size of #600 and #1000, almost constant behavior is observed when feed rate is changed from 20 mm/s to 160 mm/s.

Table 4: Results of the orthogonal experiment.

No.	Process parameter				Experiment data		
	S	W_t	a_p	V_f	MRR (mm^3/min)	Z_w	Ra (μm)
1	1	1	1	1	0.063	0.1	0.086
2	1	2	2	2	0.949	0.39	0.134
3	1	3	3	3	2.152	0.51	0.105
4	2	1	2	3	0.266	0..11	0.104
5	2	2	3	1	0.278	0.07	0.115
6	2	3	1	2	0.177	0.11	0.088
7	3	1	3	2	0.189	0.37	0.078
8	3	2	1	3	0.139	0.08	0.133
9	3	3	2	1	0.291	0.13	0.162

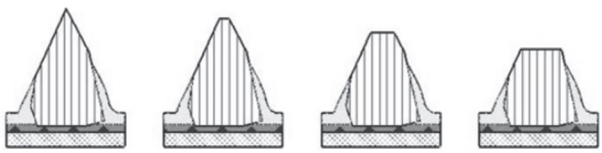

Figure 8: Wear process diagram of SiC abrasive.

In Figure 7(d), the material removal rate increased with the increase in cutting depth (a_p) from 0.1 mm to 0.5 mm as the contact area and the abrasive grains involved in polishing process increased by the increase of cutting depth, and the MRR increased.

4.1.2. On Abrasive Wear and Surface Quality. Two processes are covered by elastic abrasive wear: abrasive wear and binder breakage. The sharp top of a single abrasive grain passivated into a facet firstly in the polishing process. As the polishing continues, the facet gradually expands and becomes larger; the increased friction of the contact area results in reduced effect of abrasive cutting and increased wear of elastic abrasive. The wear process of silicon carbide abrasives has been shown in Figure 8. There is a large wear facet on the top of the abrasive grains after polishing, a small amount of abrasive particles falling off and breaking around, and serious adhesive wear [18].

As shown in Figure 9, the microscopic surface of M300 steel is polished by the ball type abrasive tool. Compared with Figure 8, it can be clearly seen that the wear process of the ball type abrasive tool is the same as that of silicon carbide, and most of the abrasive grains have a relatively smooth passivation facet on the top. In addition, the phenomenon of adhesion wear varies with the grain size. The abrasive with the grain size of #320 has more abrasive dust covered on the surface than that of #600, and the binder cannot be clearly identified. It shows that the abrasive with smaller grain size has a more serious phenomenon of abrasive dust adhesion in polishing, which will influence the effect of surface polishing of the workpiece.

As shown in Figure 10(a), in general, abrasive wear (M_t) increased with the increase in grinding speed (w_t) from 1500 r/min to 12000 r/min except the wear of #320 abrasives, for which the abrasive wear first decreases and then slightly increases. As the grain size of #320 abrasive tool is much larger than the #600 and #1000 abrasive tools, the single abrasive grain suffers a large pressure and causes a large degree of wear. However, the phenomenon was reduced when the grinding speed was greater than 6000 r/min.

In Figure 10(b), abrasive wear (Mt) increased with the increase in cutting depth (a_p) from 0.1 mm to 0.5 mm. Since, by the increasing of cutting depth, the amount of abrasive grain in polishing increased, the wear phenomenon aggravated, and the wear quantity increased. Under the premise of ensuring the processing efficiency and the service life of the abrasive tool, the cutting depth should be between 0.2 mm and 0.4 mm.

As shown in Figure 10(c), for the polishing process of the ball type abrasive tool, there is a critical value for the grinding speed of the abrasive tool, and the increase of the grinding speed within the critical range increased the amount of abrasive grains passing through the contact area per unit time, increased the number of effective cutting edges [12], and reduced the surface roughness of the workpiece gradually. After the grinding speed was greater than 7500 r/min, the higher tangential linear velocity of the workpiece would heighten the temperature between the abrasive tool and the workpiece. At this time, the wear of the binding agent was intensified, the actual cutting depth of the abrasive grain was reduced, the removal ability of the abrasive decreased [12, 19], and the downtrend of Ra slowed down and then gradually increased. Therefore, in order to obtain a good quality in polishing, the grinding speed of the elastic abrasive tool applied in this study should not exceed 9000 r/min.

A different trend is shown in Figure 10(d). The effect of cutting depth is significant on surface roughness (Ra). In general, Ra declined with the increase in cutting depth (ap) from 0.1 mm to 0.5 mm, while, for the grain size of #320 and #600, almost constant behavior is observed when cutting depth is changed from 0.2 mm to 0.3 mm.

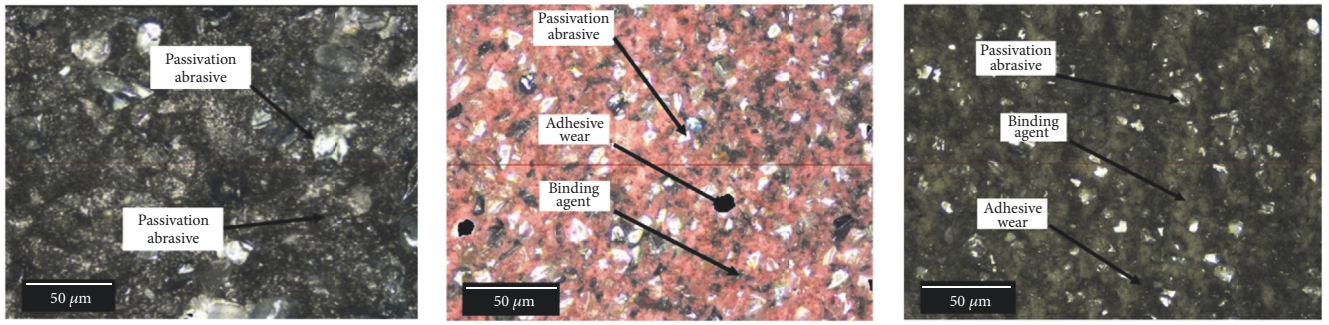

(a) #320 elastic abrasive (b) #600 elastic abrasive (c) #1000 elastic abrasive

Figure 9: Microscopic images of elastic abrasive surface after polishing.

Table 5: SNR values on surface roughness.

Process parameter		S	w_t	a_p	v_f
Level	1	19.4480	*21.8021*	19.9811	18.6353
	2	*19.8519*	17.9223	17.6423	*21.0017*
	3	19.2565	18.8321	*20.9331*	18.9195

Table 6: SNR values on material removal rate.

Process parameter		S	w_t	a_p	v_f
Level	1	*8.333*	1.367	1.000	1.667
	2	1.900	3.600	3.967	3.467
	3	6.700	*5.533*	*5.900*	*5.067*

Table 7: SNR values of parameters on wear ratio.

Process parameter		S	w_t	a_p	v_f
Level	1	-11.34	-15.94	*-20.37*	*-20.27*
	2	*-20.48*	*-17.74*	-15.02	-11.99
	3	-16.1	-14.25	-12.53	-15.65

4.2. Optimization of Grinding Parameters

4.2.1. Optimization of Experimental Results. The surface roughness, material removal rate, and wear ratio were regarded as targets, and the signal-to-noise (SNR) ratio analysis was performed on the experimental data. The results are presented in Tables 5–7. The order of influence level of the controllable factors to the surface roughness, in sequence, can be listed as factors B (spindle speed), D (feed rate), C (cutting depth), and A (grinder size) (i.e., 21.8021 > 21.0017 > 20.9331 > 19.8519). Table 6 shows the influence level of each factor on material removal rate, while Table 7 indicates the level of influence of each factor on the wear ratio.

In order to achieve high-efficiency and high-quality polishing, the multiobjective optimization ideas were employed in this paper. The theory of Grey systems is a technique for performing prediction, relational analysis, and decision-making in many areas [2] . The Grey relational analysis method, which establishes a mathematical relationship model among factors according to the behavioral characteristic data, can solve the design problem of multiobjective optimization [20].

According to the experimental results in Table 4, considering the different definition and quantity units of each optimization objective, the three groups of data as sequence data need to be normalized:

(1) The material removal rate and wear ratio are considered to be positive indicators, and the dimensionless formula is

$$z_i^*(j) = \frac{z_i^0(j) - \min z_i^0(j)}{\max z_i^0(j) - \min z_i^0(j)} i \quad (i = 1, 2, 3 \ldots, 9;\ j = 1, 2, 3) \tag{7}$$

(2) The surface roughness is considered to be a negative indicator, and the dimensionless formula is

$$z_i^*(j) = \frac{\max z_i^0(j) - z_i^0(j)}{\max z_i^0(j) - \min z_i^0(j)}, \tag{8}$$

where $z_i^0(j)$ represents the reference sequence, which is the ideal standardized result of the ith experiment under the jth performance characteristic; $z_i^*(j)$ represents the comparison sequence, which is the actual normalized experimental result

The weight coefficient matrix $\{0.2297, 0.1220, 0.6483\}^{\mathrm{T}}$ of surface roughness, material removal rate, and wear ratio was obtained by an analytic hierarchy process. In order to obtain a better combination of each individual optimization target, the correlation coefficient of the corresponding element between each comparison sequence and reference sequence can be calculated by the following equation and the processing result is shown in Table 8:

$$\xi_{i,j} = \frac{\min_i \min_j \left|z_i^0(j) - z_i^*(j)\right| + \rho \max_i \max_j \left|z_i^0(j) - z_i^*(j)\right|}{\left|z_i^0(j) - z_i^*(j)\right| + \rho \max_i \max_j \left|z_i^0(j) - z_i^*(j)\right|}, \tag{9}$$

where $\xi_{i,j}$ is the correlation coefficient between the jth target in the reference sequence $z_i^0(j)$ and the ith comparison sequence, and its value reflects the weight of $\max_i \max_j |z_i^0(j) - z_i^*(j)|$ and the indirect influence of each

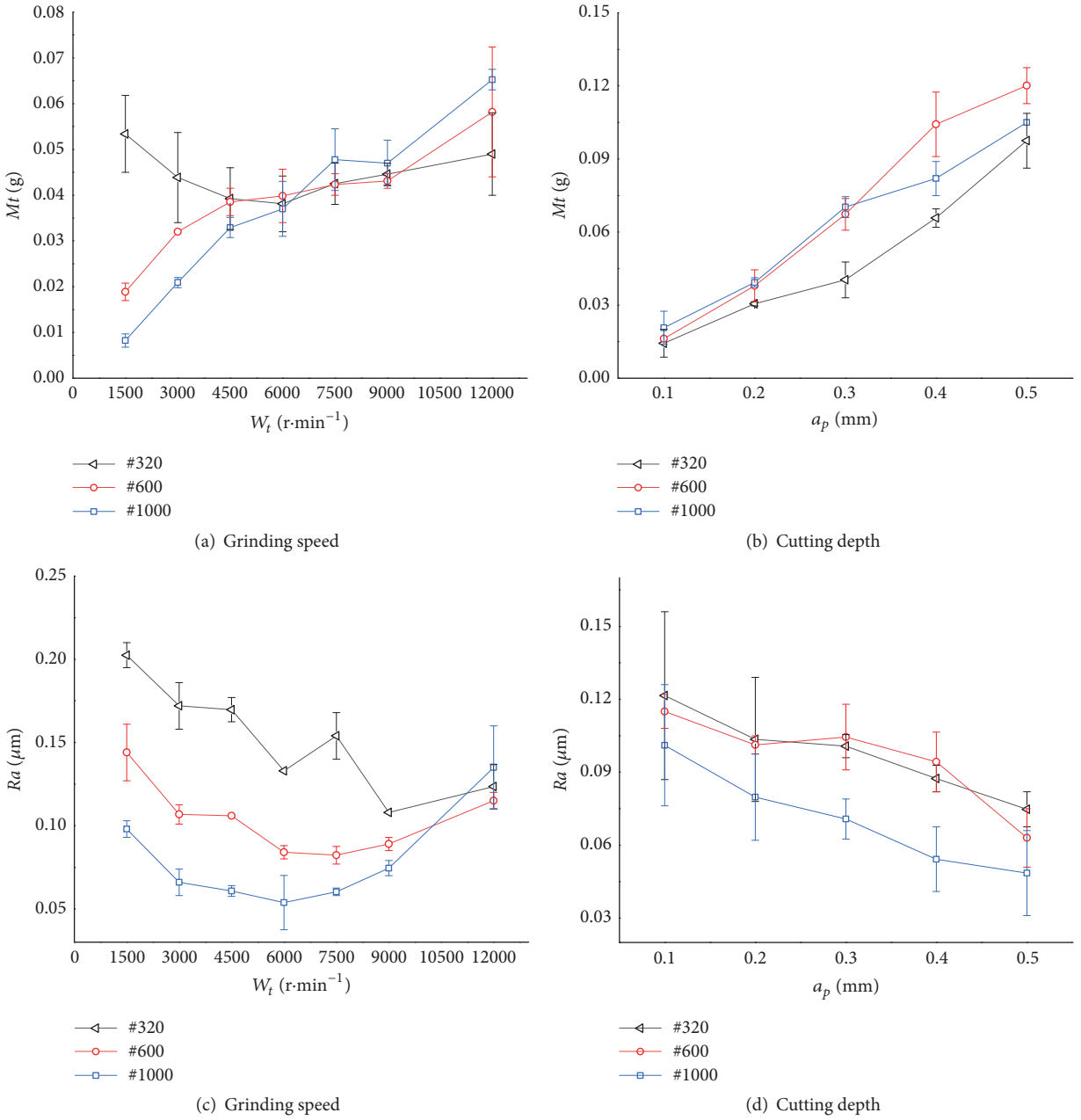

Figure 10: Plots of parameters' effect on abrasive wear and surface quality.

Table 8: Grey correlation coefficient of each experimental scheme.

Test No.	Grey correlation coefficient		
	Material removal rate	Wear ratio	Surface roughness
1	0.3333	0.3492	0.4016
2	0.3579	0.3333	0.5204
3	0.3595	0.3667	1
4	0.3459	0.3548	0.4080
5	0.4648	0.6471	0.6456
6	0.3474	0.6111	0.3333
7	0.3416	0.3385	0.6375
8	0.3564	0.3548	0.4679
9	1	1	0.4722

Table 9: Grey correlation degree of each experimental scheme.

Test No.	Processing parameters				Grey correlation degree
	Grain size	Grinding speed	Cutting depth	Feed rate	
	S	w_t	a_p	v_f	(GRC)
1	1	1	1	1	0.5508
2	2	2	3	1	0.4365
3	3	3	2	1	0.3465
4	2	3	1	2	0.5439
5	1	2	2	2	0.4933
6	3	1	3	2	0.8331
7	3	2	1	3	0.3881
8	2	1	2	3	0.4757
9	1	3	3	3	0.6148

Table 10: Mean GRC values of the target function.

Process parameter	S	W_t	Ap	V_f
Level 1	*0.0529*	*0.6199*	0.4943	0.4446
Level 2	0.4854	0.4393	0.4385	*0.6234*
Level 3	0.5226	0.5017	*0.6281*	0.4929
Range value	0.0675	0.1806	0.1896	0.1788

factor on the correlation degree; ρ is identification coefficient with its value in [0, 1], generally 0.5.

After obtaining the Grey correlation coefficient, the weighted average of the correlation coefficients can be obtained by (10) because each index plays a different role in the comprehensive evaluation. The calculation results of the Grey correlation degree (GRC) of each experimental scheme are shown in Table 9.

$$\eta_{\mathrm{i}} = \frac{1}{n}\sum_{k=1}^{n} \lambda_k \xi_{i,j}\mathrm{i}, \tag{10}$$

where η_{i} is the Grey relational grade for the ith experiment; λ_k is the weight coefficient.

The average Grey correlation degree of S, $\mathrm{W_t}$, $\mathrm{A_p}$, and $\mathrm{V_f}$ was analyzed by orthogonal extreme difference analysis, and the influence degree of each factor on the experimental results was analyzed. The average Grey correlation degree of each parameter is shown in Table 10. It can be noticed that the selected design parameter was A1B1C3D2 according to the orthogonal analysis. For the multiobjective optimization, the impact levels were sorted in the descending order, that is, in the order of the design parameters C, B, D, and A.

4.2.2. Optimization of Parameters' Interval of Surface Polishing. The polishing mechanism of the ball type abrasive tool is more complicated, and there is still no unified consensus on the selection of grinding and polishing parameters. Moreover, there is an interaction between the optimization targets in actual production. In this paper, based on the orthogonal experiment, the range of each parameter interval was optimized and the process parameters were studied. For the multiobjective optimization problem, the sensitivity analysis method was used to transform the multiobjective optimization problem into a single-objective optimization problem to seek the Pareto solution of the multiobjective. The power function model is used for regression analysis on experimental data, as shown in

$$\begin{aligned} \mathrm{Ra} &= k_1 S^{b_1} \omega_t^{\,b_2} a_p^{\,b_3} V_f^{\,b_4} \\ MRR &= k_2 S^{c_1} \omega_t^{\,c2} a_p^{\,c3} V_f^{\,c_4}, \end{aligned} \tag{11}$$

where $\mathrm{K_1}$ and $\mathrm{K_2}$ are the proportional coefficient; $\mathrm{b_1}$ and $\mathrm{c_1}$ are nonlinear exponential power.

The logarithm of both sides of the formula is taken at the same time, the regression parameters are calculated by the least squares method to obtain the estimated value, and a multiple linear regression equation is established:

$$\begin{aligned} y_1 &= -2.4202 + 0.01S + 0.323\omega_t + 0.008a_p \\ &\quad - 0.0608V_f \\ y_2 &= -2.1053 - 1.419S + 0.739\omega_t + 0.911a_p \\ &\quad + 0.411V_f. \end{aligned} \tag{12}$$

The prediction models of Ra and MRR were obtained as follows:

$$Ra = 0.0038S^{0.01}\omega_{\mathrm{t}}^{\,0.323}\mathrm{a_p}^{\,0.008}\mathrm{V_f}^{\,-0.0608} \tag{13}$$

$$MRR = 124.771S^{-1.419}a_p^{\,0.739}\omega_{\mathrm{t}}^{\,0.911}\mathrm{V_f}^{\,0.411}. \tag{14}$$

For the significance test of the predictive model, the confidence interval of Ra was (-0.148, 0.145) and the correlation coefficient $\mathrm{r^2}$ was 0.8172, while the confidence interval of MRR was (-0.56, 4.220) and the correlation coefficient $\mathrm{r^2}$ was 0.9601. The correlation coefficients of the two groups were close to 1, F=168.56, $\mathrm{P=3\times10^{-6}}$ <<0.05; the regression model was proved to be significant.

According to the empirical formula of the surface roughness and material removal rate of the surface polishing

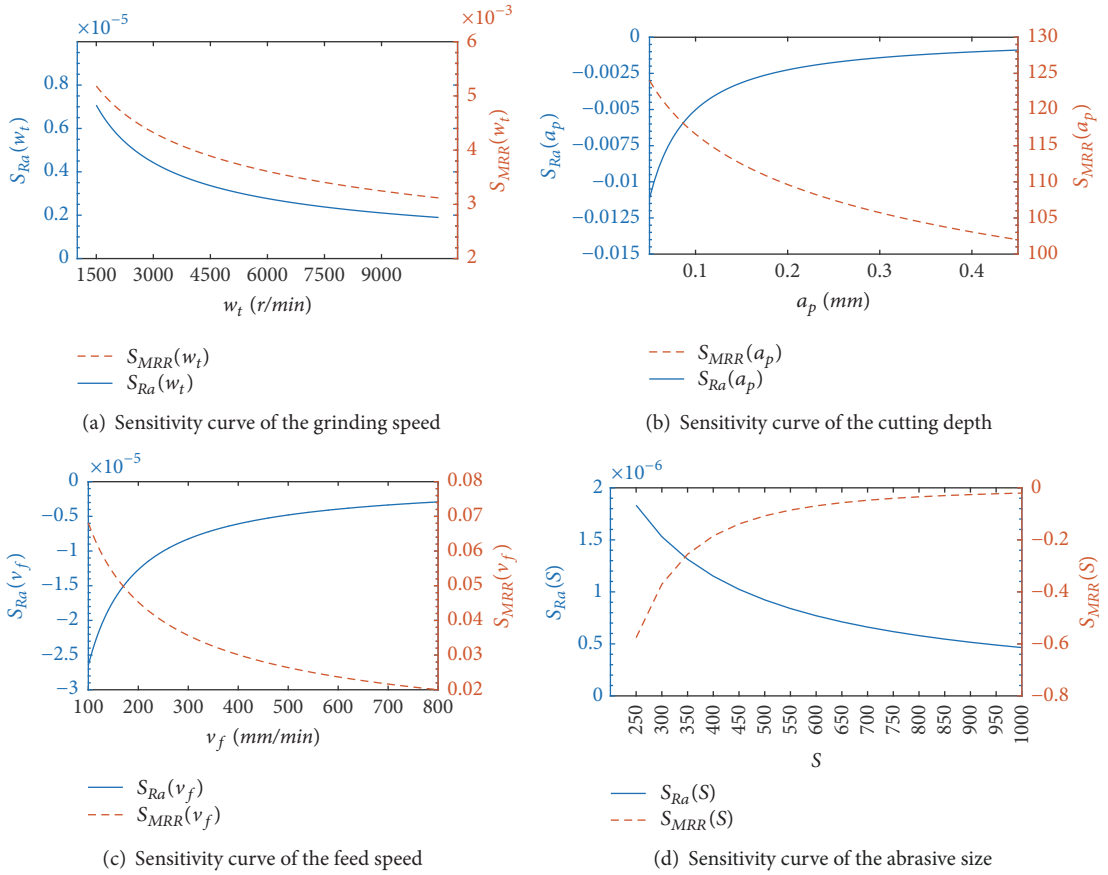

Figure 11: Sensitivity curve of the grinding parameters.

obtained in the foregoing, and formula (11), the sensitivity model of the surface roughness and the material removal rate to parameters of each polishing model can be obtained as follows:

$$\begin{aligned} S_{Ra}^{\omega_t} &= 1\times10^{-3}\omega_t^{-0.677}a_p^{0.008}V_f^{-0.0608}S^{0.01} \\ S_{Ra}^{a_p} &= -3\times10^{-5}\omega_t^{0.323}a_p^{-0.992}V_f^{-0.0608}S^{0.01} \\ S_{Ra}^{V_f} &= -2\times10^{-4}\omega_t^{0.323}a_p^{0.008}V_f^{-1.0608}S^{0.01} \\ S_{Ra}^{S} &= 3.8\times10^{-5}\omega_t^{0.323}a_p^{0.008}V_f^{-0.0608}S^{-0.99} \end{aligned} \tag{15}$$

$$\begin{aligned} S_{MRR}^{\omega_t} &= 92.206\omega_t^{-0.261}a_p^{0.911}V_f^{0.411}S^{-1.419} \\ S_{MRR}^{a_p} &= 113.666\omega_t^{0.739}a_p^{-0.089}V_f^{0.411}S^{-1.419} \\ S_{MRR}^{V_f} &= 51.281\omega_t^{0.739}a_p^{0.911}V_f^{-0.589}S^{-1.419} \\ S_{MRR}^{S} &= -177.05\omega_t^{0.739}a_p^{0.911}V_f^{0.411}S^{-2.419}. \end{aligned} \tag{16}$$

Within the range of experimental parameters, the average grinding speed was w_t=6000 r/min, and the average cutting depth was a_p=0.25 mm. Under the condition that the feed rate is 80 mm/s and the grain size is #600, the absolute sensitivity model of the surface roughness Ra was

$$\begin{aligned} S_{Ra}^{\omega_t} &= 7.324\times10^{-4}\omega_t^{-0.677} \\ S_{Ra}^{a_p} &= -3.5343\times10^{-4}a_p^{-0.992} \\ S_{Ra}^{V_f} &= -3.502\times10^{-3}V_f^{-1.061} \\ S_{Ra}^{S} &= 4.336\times10^{-4}S^{-0.99}. \end{aligned} \tag{17}$$

The absolute sensitivity model of the material removal rate MRR was

$$\begin{aligned} S_{MRR}^{S} &= -15.377S^{-2.419} \\ S_{MRR}^{\omega_t} &= 3.496\omega_t^{-0.261} \\ S_{MRR}^{a_p} &= 94.992ap^{-0.089} \\ S_{MRR}^{V_f} &= 1.026V_f^{-0.589}. \end{aligned} \tag{18}$$

According to the model above, the sensitivity curves of surface roughness and material removal rate to grain size, cutting depth, feed rate, and grinding speed are obtained as shown in Figure 11. Generally, Ra is most sensitive to the change of cutting depth, and MRR is most sensitive to the

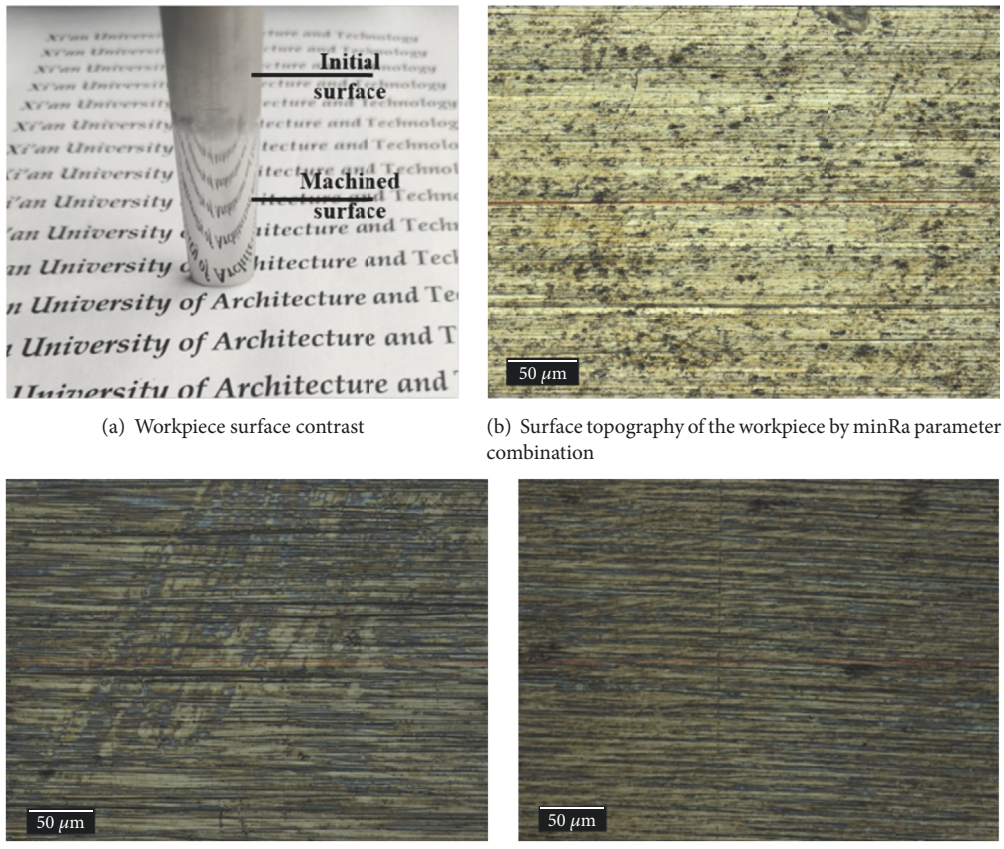

(a) Workpiece surface contrast

(b) Surface topography of the workpiece by minRa parameter combination

(c) Initial surface topography

(d) Surface topography of the workpiece after polishing

Figure 12: Surface topographies of the workpiece by optimized parameters before and after polishing.

change of cutting depth and feed rate. In Figure 11, it can be seen that, for the grinding speed, the sensitivity range of Ra is divided into three sections: [1500 4500], [4500 7500], and [7500 9000]. The sensitivity of [1500, 4500] is the largest, and Ra is affected significantly by the cutting depth in this range. The curve of the cutting depth is gentle in the range of [0.2, 0.4], and the sensitivity changes slowly while the feed rate is in the [300, 500] interval, indicating that the surface roughness does not change significantly in this interval.

In general, the MRR is most sensitive to the feed rate and cutting depth. The sensitivity is relatively large when the feed rate is within [20, 80], the cutting depth [0.1, 0.2], or the grain size [400, 1000], and the amplitude of sensitivity change is relatively flat while the grinding speed is greater than 4500 r/min.

The stable domains and unstable domains within the experimental parameters can be obtained according to the parameters of Figure 9. The variation of surface roughness of each grinding parameter within the total interval can be obtained by the analysis of orthogonal experimental data, as shown in Table 11.

Considering the acquisition of stable surface roughness in the actual processing while ensuring the high material removal rate, the preferred interval as shown in Table 12 is determined. The preferred interval of grinding speed is in the middle section of stable domains of the material removal; the preferred interval of cutting depth, grain size, and feed rate is in the unstable domain.

Table 11: Mean Ra of each parameter level.

Process parameter	S	ω_t	a_p	v_f
Level 1	0.108	0.083	0.102	0.121
Lever 2	0.102	0.127	0.133	0.094
Level 3	0.118	0.118	0.093	0.114

4.2.3. Experimental Verification. As shown in Table 4, the selected design parameter of single target was A2B1C3D2, and the better design parameter of multiobjective was A1B1C3D2. Repeated comparison experiments were performed on the two groups, respectively; the average material removal rates of minRa and multiobjective combination were 3.9 mg/min and 1.5 mg/min, and the wear ratios were 0.6 and 0.4.

The comparison of the M300 surface topographies at the beginning and the end of the experiment multiobjective optimization combination has been shown in Figures 12(c)

Table 12: Grinding parameter preferred interval.

Process parameter	Optimization interval	Stability	Surface roughness trend
S	[300 600]	Unsteady	0.102-0.108
ω_t (r/min)	[4500 7500]	Stable	0.083-0.118
a_p (mm)	[0.1 0.3]	Unsteady	0.093-0.102
v_f (mm/s)	[20 80]	Unsteady	0.094-0.121

and 12(d), in which it has been shown that the milling texture is greatly reduced and the surface damage is improved. Figure 12(a) shows the workpiece surface contrast before and after machining. The surface roughness after processing was 0.056 μm. Compared with the surface appearance of the minRa parameter combination shown in Figure 12(b), the material removal rate was improved by 2.6 times, and the overall processing technology is greatly improved, indicating that the parameter optimization method is effective.

5. Conclusion

In this study, based on the theoretical analysis of material removal function of the ball head abrasive tool, the influence law of process parameters in the polishing process of M300 steel and the parameter optimization prediction method were studied to achieve high-efficiency and high-quality polishing. The main conclusions are drawn as follows:

(1) Based on the Preston equation, the material removal equation of the ball head abrasive tool under convex contact conditions is deduced, and the Preston coefficient in the theoretical model is modified and analyzed, which provided a theoretical basis for the study of abrasive polishing by an elastic grinding tool

(2) Multiobjective optimization plays an important guiding role in the selection of polishing parameters. Compared with the single-objective optimization results, the surface appearance of the material under the multiobjective optimization combination has been greatly improved, the material removal rate has been increased by 2.6 times, and the surface roughness has reached the mirror requirements

(3) The optimization interval to meet the requirements of obtaining stable surface roughness in actual processing and ensuring a higher material removal rate was determined. Also authors are encouraged to refine the range of polishing parameters to address more complex issues, such as meeting higher processing requirements and reducing wear and tear on the abrasive tool. It is also noticed that the proposed research ideas can also be used in the grinding and polishing analysis of related materials, including the theoretical and technological analysis of surface polishing of titanium alloys and other alloys by elastic abrasives

Data Availability

The data used to support the findings of this study are included within the article.

Conflicts of Interest

The authors declare that they have no conflicts of interest.

Acknowledgments

This research was supported by the National Natural Science Foundation of China (51375361).

References

[1] J. S. Fang and S. C. Hong, "Ultra-precision surface finish of the hardened stainless mold steel using vibration-assisted ball polishing process," *The International Journal of Machine Tools and Manufacture*, vol. 48, no. 7-8, pp. 721–732, 2008.

[2] N. Tosun, "Determination of optimum parameters for multi-performance characteristics in drilling by using grey relational analysis," *The International Journal of Advanced Manufacturing Technology*, vol. 28, no. 5-6, pp. 450–455, 2006.

[3] K. H. Hashmi, G. Zakria, M. B. Raza et al., "Optimization of process parameters for high speed machining of Ti-6Al-4V using response surface methodology," *The International Journal of Advanced Manufacturing Technology*, vol. 85, no. 5-8, 2015.

[4] P. J. Liew, A. Shaaroni, N. A. C. Sidik, and J. Yan, "An overview of current status of cutting fluids and cooling techniques of turning hard steel," *International Journal of Heat and Mass Transfer*, vol. 114, pp. 380–394, 2017.

[5] X.-L. Zhou, "Experimental and optimization study of YG8 cemented carbide high speed grinding process," Hunan University, 2011.

[6] Y.-J. Zhan, "Mechanism of high-speed grinding of cemented carbide by ceramic bond diamond grinding wheel," Huaqiao University, 2013.

[7] J. Li, J.-B. Zhao, L.-R. Guan et al., "Research on grinding and polishing process of spherical polishing tools," *Aviation Precision Manufacturing Technology*, vol. 51, no. 6, pp. 5–8, 2015.

[8] F. Klocke, D. Novovic, A. Elfizy et al., "Abrasive machining of advanced aerospace alloys and composites," *CIRP Annals - Manufacturing Technology*, vol. 64, no. 2, pp. 581–604, 2015.

[9] S. Zeng and L. Blunt, "Experimental investigation and analytical modelling of the effects of process parameters on material removal rate for bonnet polishing of cobalt chrome alloy," *Precision Engineering*, vol. 38, no. 2, pp. 348–355, 2014.

[10] V. S. Sooraj and V. Radhakrishnan, "Fine finishing of internal surfaces using elastic abrasives," *The International Journal of Machine Tools and Manufacture*, vol. 78, pp. 30–40, 2014.

[11] W. Wei, "Research on progressive softening abrasive grain grinding wheel finishing," 2016.

[12] Z.-K. Xu, "Research on automatic mechanical polishing technology and the process optimization for stainless steel thin-wall material workpieces," Huazhong University of Science and Technology, Wuhan, China, 2012.

[13] F. W. Preston, "The theory and design of glass plate polishing machine," *Journal of the Society of Glass Technology*, vol. 11, pp. 214–257, 1927.

[14] L. P. Valenti, *Contact Mechanics and Friction Physical Principles and Applications*, vol. 2, Tsinghua University Press, Beijing, China, 2011.

[15] Y. Lu and Y. Huang, "Experimental investigation in the grinding and wear performance of abrasive belt grinding," *Mechanical Science and Technology*, vol. 33, no. 12, pp. 1865–1867, 2014.

[16] J. Li, "Theoretical and experimental research on precision grinding and polishing technology for complex surfaces," Shenyang Ligong University, 2016.

[17] X.-J. Wu, X.-Z. Yu, R.-P. Liu et al., "Experimental study on flexible abrasive grinding of M330 steel," *Nanotechnology and Precision Engineering*, vol. 13, no. 3, pp. 199–204, 2015.

[18] Y. Huang, C. Yang, and Z. Huang, "Experimental research on abrasive belt grinding for 304 stainless steel," *Chinese Journal of Mechanical Engineering*, vol. 22, no. 3, pp. 291–295, 2011.

[19] J. Xie, J.-X. Sun, Y.-H. Li et al., "Precision and mirror grinding of F-Theta free-form surface lens," *Journal of Mechanical Engineering*, vol. 52, no. 17, pp. 72–77, 2016.

[20] S.-M. Ji, W. Wei, M.-S. Jin et al., "Mold finishing for multi-factor and muti-objective," *China Mechanical Engineering*, vol. 27, no. 20, pp. 2802–2806, 2016.